Gate bias polarity dependent H migration and O vacancy generation through Si=O–H complex formation in SiO_2/Si(100)

Koichi Kato*

Advanced LSI Technology Laboratory, Toshiba Corporate Research and Development Center, 1 Komukai Toshiba-cho, Saiwai-ku, Kawasaki 210-8582, Japan

(Received 2 August 2011; revised manuscript received 21 November 2011; published 15 February 2012)

We studied H-atom migration in SiO_2/Si systems triggering O vacancy generation based on first-principles calculations. The migrating H atoms in SiO_2 have been found to be mostly negatively charged irrespective of the charge-state polarity in the systems because strong charge transfer from the Si to the O atoms substantially increases the O $2p$ energy levels. Although the SiO_2 systems with no defect are not degraded by the migrating H atoms, 2Si=O–H complex formation in the SiO_2/Si systems has been found to generate an O vacancy via H_2O molecule desorption after alternate electron transfer between the 2Si=O–H complex and the Si substrate, leading to the final electrical breakdown of SiO_2 films. The migration of negatively charged H atoms and their degradation agree well with the recently observed gate bias polarity dependent SiO_2 film degradation.

DOI: 10.1103/PhysRevB.85.085307 PACS number(s): 73.20.−r, 73.22.−f, 73.40.Ty, 73.43.Cd

I. INTRODUCTION

As downscaling of electronic devices in large-scale integration (LSI) technology approaches the scaling limit, sustainable reliability of electronic devices is becoming more important. Since impurity diffusion and atom mixing have to be confined within a nanometer-order space, processing temperatures for SiO_2 films such as oxidation and annealing must be reduced. Consequently, substantial amounts of defects remain in the SiO_2 films, especially at the interfaces, after the oxidation or annealing processes.[1–5] Hydrogen-termination techniques have played decisive roles through several decades in regaining reliability of semiconductor devices.[6–9] With forming gas annealing in hydrogen ambient at moderately high temperatures, H_2 molecules are dissociated and H atoms terminate dangling bonds (DBs) at the interface layer or in a Si substrate,[10] leading to reduction of defect-oriented flatband voltage (Vfb) shifts and to improvement of carrier mobility.[11] However, greater application of annealing processes in hydrogen ambient results in generation of hydrogen-induced defects.[1,12] Negatively charged traps are generated following charge injection into SiO_2 films.[13] Even without this hydrogen ambient annealing, hydrogen atoms subsequently penetrate SiO_2 films through fabrication of overlayer films. As a consequence of more frequent application of chemical vapor deposition (CVD) techniques for overlayer film formation at lower temperatures, large amounts of H atoms are left in fabricated film layers after the CVD process, and these H atoms migrate into the underlying SiO_2 film during the CVD process or subsequent processes, causing degradation even at low temperatures.

H atoms are known to have several stable positions in a SiO_2 system. H atoms form a 2Si=O–H complex with a threefold coordinated oxygen atom when the system is positively charged, whereas they form a Si–H bond when the system is negatively charged.[14–16] Even in a neutral SiO_2/Si system, a H atom participates in threefold coordination of the oxygen atom, forming a 2Si=O–H complex inside the SiO_2 film fabricated on the Si substrate with electron tunneling to the Si substrate.[17] Proton transfer has been considered to be a mechanism that explains H hopping between stable sites and formation of the H-participating complex in the SiO_2 system. This is because the positively charged $(\alpha\text{-quartz})^{1+}$ is more stable than $(\alpha\text{-quartz})^{1-}$ as the Fermi level decreases from the top of the conduction band toward the valence band.[14,16,18,19] This idea is not in agreement with recent experimental findings on the reliability of p-FETs (field effect transistors) fabricated with gate stacks.[20] Under negative gate biases, H atoms seem to migrate toward the Si substrate, where degradation of the interfacial SiO_2 layer starts. H atoms degrade reliability of SiO_2 films more severely than negative bias temperature instability (NBTI) does since this degradation can be greatly ameliorated by reduction of H atom concentration in high-k films. Under positive gate biases for n-FETs, however, this degradation is not obvious. H atoms seem to be negatively charged rather than positively charged in the interfacial SiO_2 layers and the high-k films because of the gate bias polarity dependent migration. The confused understanding may arise from the fact that the energy level of O $2p$ is slightly lower than that of H $1s$ isolated in a vacuum. In an actual SiO_2 system, however, electronic charge transfer from a Si to an O atom enhances electronic concentration around O atoms. Then, the energy level of O $2p$ rises substantially because of energy increase due to Coulomb repulsion among several O $2p$ states hybridized with Si atoms. As a result, the top of the SiO_2 valence band, which has a more oxygen character, reaches −9.0 eV from the vacuum level, lying far above the isolated H $1s$ level of −13.6 eV. Electronic charge transfer will occur from O atoms to H atoms in the SiO_2 system, whether strong hybridization of H $1s$ and O $2p$ states occurs or not. This suggests that the actual effective charge of H atoms may not depend on the charge-state polarity of the total SiO_2 system. Accordingly, it is necessary to know the gate bias polarity dependence of H-atom migration under applied electric fields, and whether H-atom participation in the SiO_2 network leads to degradation of the SiO_2 network.

This study is intended to clarify the H-atom migration mechanism in SiO_2[21] and SiO_2/Si systems, and explore the H-atom-induced degradation mechanism. Given that the behaviors of H atoms have been thoroughly studied,[15,22] we performed first-principles calculations for H-atom migration in the SiO_2 and SiO_2/Si structures with varying charge-state

polarity, where the effective charge on the H atom is examined at each migration step.[23] In this way, the deterioration of the SiO_2 network by migrating H atoms is explored.

II. CALCULATION METHODS

The aim of the present study is to understand the H migration under electric fields and the mechanism of H-induced degradation based on first-principles theoretical calculations. Our calculations are based on density functional theory (DFT) and the generalized gradient approximation (GGA) of PW91 in order to describe hydrogen and oxygen properties properly.[24] We used the original version of the PHASE code.[25] The calculations were performed using ultrasoft pseudopotentials[26] for hydrogen and oxygen atoms with 1 k to 4 k points for Brillouin-zone samplings. We found that the cutoff energies of 25 Ry for the wave functions and 144 Ry for the augmented electron densities are sufficient for converging electronic calculations.[3] In the present study, the calculations were performed with a thick SiO_2 film region and with a SiO_2/Si interface region, separately. Since we do not take into account band offsets, the H-migration mode change from the SiO_2 to the SiO_2/Si interface is beyond the scope of this work. The structure of the thick SiO_2 film is represented by an α-quartz consisting of a ($2 \times 2 \times 2$) unit cell with periodic boundary conditions. The SiO_2/Si interface structure is prepared by inserting O atom into a Si–Si bond from a topmost surface to deeper regions on a repeated slab modified from a $c(4 \times 2)$ surface unit cell consisting of 14 layers of Si atoms and a vacuum spacing with the same thickness. The oxidized layers are relaxed accordingly to be in equilibrium positions. Inversion symmetry with respect to the slab center located at a Si bond center is used for the interface to increase the computational efficiency.

The total density of states (TDOS) for the systems and local density of states within the Wigner-Seitz cell (LDOS) are evaluated. An effective charge of valence electrons for each atom is also evaluated by summing electronic charge densities within its Wigner-Seitz cell, which can be calculated at grid points generated regularly on Cartesian coordinates. In particular, the charge density defined at each grid point belongs to the atom closest to the grid point.[24] Since this charge assignment technique may not be accurate enough for smaller H atoms, the effective electronic charges are analyzed by comparing the components of occupied and unoccupied states in the LDOS, whose orbits can be identified in a real space. Furthermore, the effective charges have been also evaluated by Mulliken charge based on the space of atomic orbital sets for typical structures by using GAUSSIAN09. Although the Mulliken charge in a negatively charged H atom is underestimated because of substantial wave function expansion, it could provide the lowest limit for the effective electronic charge.

III. RESULTS

A. Charge-state polarity dependence of H migration in SiO_2

The equilibrium position of a H atom in a neutral α-quartz was found to be the midcenter of the interstice with slight structure expansion of surrounding host Si and O atoms [Fig. 1(a)], as reported previously.[14,15] The structure optimization does not exhibit strong orbital hybridization between the H atom and the SiO_2 host. Figure 1(b) shows the TDOS for the SiO_2 system (upper) and LDOS for the H atom (lower). The LDOS (up-spin indicated by blue lines and down-spin indicated by red lines) is split into three strong sharp peaks. The higher up-spin state 2 is occupied whereas the much higher down-spin state 3 is unoccupied above the Fermi level. The lower peak 1 is hybridized with the host SiO_2 states, and the hybridized up- and down-spin states are located lower than the top of the SiO_2 valence band. Charge transfer occurs from the occupied state in the SiO_2 host to the lower hybridized states. These occupied peaks 1 and 2 for up-spin states are displayed by the yellow isosurfaces of the electronic charges of states at the H atom, as shown in Figs. 1(c) and 1(d), clearly indicating that both peaks originate in the H atom. Hereafter, the electronic charges will be displayed only for up-spins when both up- and down-spin states are degenerated. The effective charge on the H atoms is evaluated to be a negative value of -0.40. In comparison to GGA, the effective charge on the H atom with the same geometry was also calculated to be -0.40 for LDA. This value may have been overestimated because of the use of the Wigner-Seitz cell for a small H atom. The unoccupied main peak is, however, smaller than the occupied peak, and the occupied down-spin component of H $1s$ states is also involved in the effective charge for the H atom, as clearly seen in the LDOS. Taking these effects into account, the effective charge of the H atom will still be a negative value. The effective charge evaluated in the same atomic geometry of the central region in Fig. 1(a) by the Mulliken charge with the $HSi_{18}O_{22}$ cluster by terminating 28 Si DBs with H atoms was also a negative value of -0.17. The effective charge of the H atom is definitely negative. The migration of the H atom occurs through the interstice of the α-quartz with an energy barrier of less than 0.13 eV.

Next, we examine H-atom migration in a positively charged $(\alpha\text{-quartz})^{1+}$. Here, $(\alpha\text{-quartz})^{1+}$ denotes that one electron is extracted from the α-quartz. The positive charge has been compensated by a uniform negative background charge to avoid the divergence. The optimization of atomic positions leads to orbital hybridization between the H atom and one of the O atoms in the host SiO_2, as shown in Fig. 2(a). A threefold coordinated configuration appears at the O atom when the electronic structure of the O atom forms an $sp^2 + p_z$ configuration from 5 valence electrons with one electron exception close to a N atom. Figure 2(b) shows the TDOS for the SiO_2 system (upper) and LDOS for the initial H atom (lower). The up- and down-spin states (blue lines) are fully degenerated and are split into almost 6 peaks for occupied and unoccupied states in the LDOS through strong hybridization with the host O states. The electronic charges of states at the H atom for the main two occupied peaks (1 and 2) are displayed by yellow isosurfaces in Figs. 2(c) and 2(d), respectively, clearly indicating these states are bonding states between the H $1s$ and O $2s$ states, and between the H $1s$ and O $2p$ states, respectively. These bonding states (peaks 1 and 2) are mostly located at the energies much lower than the top of the SiO_2 valence band. The lowest peak located at as low as -22 eV from the Fermi level is lower than the O $2s$ states presumably because the positively charged $(2Si{=}O{-}H)^{1+}$ complex further lowers the electronic states

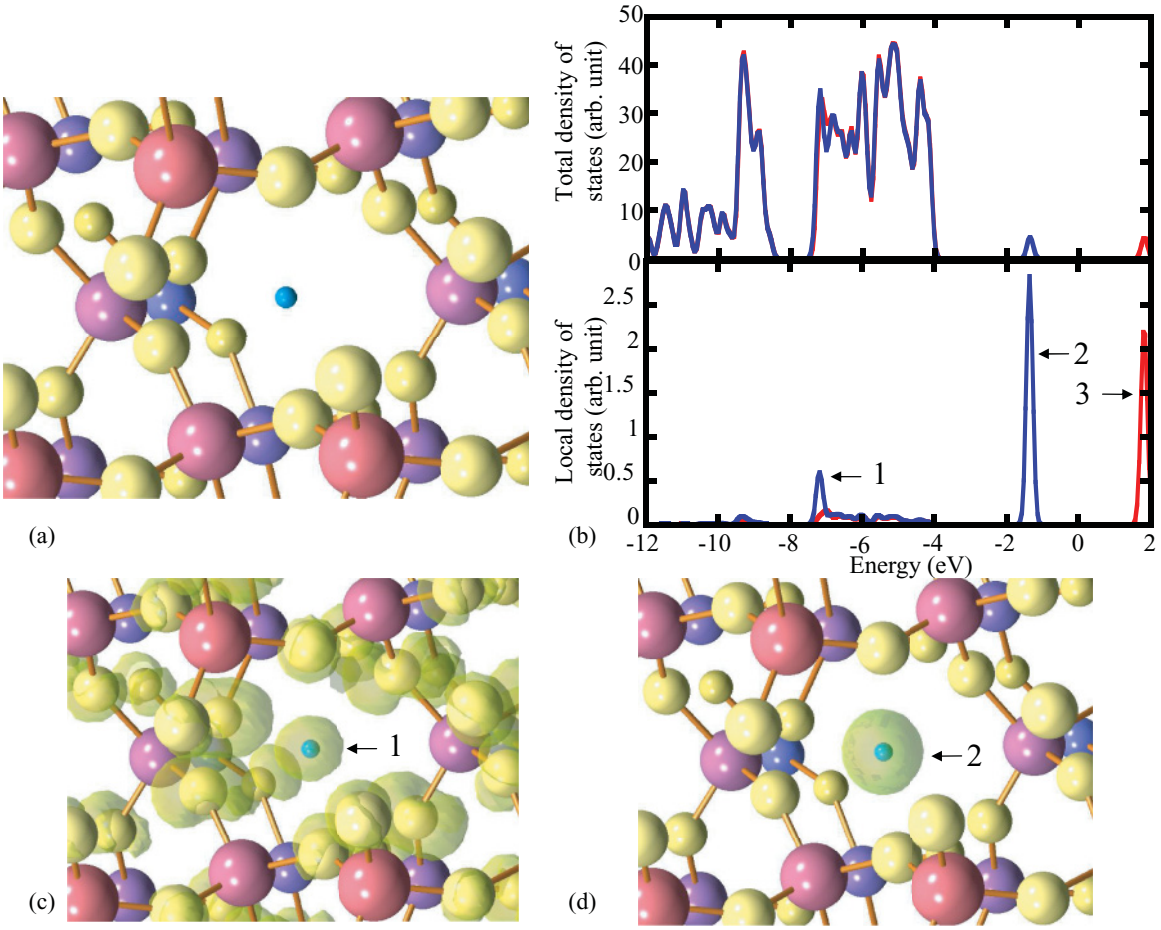

FIG. 1. (Color online) (a) The equilibrium position of the H atom in a neutral α-quartz. Large balls represent Si atoms from red to blue according to the depth. Small blue and white balls represent H and O atoms, respectively. (b) TDOS for the SiO_2 system (upper) and LDOS for the H atom (lower). Up- and down-spin states are drawn by blue and red lines, respectively. (c), (d) Yellow isosurfaces represent the electronic charges of states corresponding to peaks 1 and 2 in (b).

at the H atom. On the other hand, the electronic charges of states at the H atom for the two unoccupied states (peaks 3 and 4) are displayed by blue isosurfaces in Figs. 2(e) and 2(f), respectively, clearly indicating that these states are antibonding states between H 1s and O 2s states, and between H 1s and O 2p states. Although the positively charged $(\alpha\text{-quartz})^{1+}$ is more stable than $(\alpha\text{-quartz})^{1-}$ with lowering of the Fermi level, the effective charge on the H atom in this case is evaluated to be still a negative value of -0.41. This value may also have been negatively overestimated because of the small H atom. Hence, integration of the LDOS along energy for both spins is calculated to be 2.48, larger than 2.0, implying the orbital components from the other atoms. Comparing the occupied components of 1.41 and the unoccupied components of 1.07, the effective charge of the H atom seems to be still negative, where the components from the other orbits are considered to be involved at almost the same rate. This means that electronic charges have transferred from the SiO_2 host to the orbital hybridized H atom, not from the H atom to the SiO_2 host. On the other hand, the effective charge evaluated in the same atomic geometry for the central region in Fig. 2(a) by the Mulliken charge with the $(HSi_{18}O_{22})^{1+}$ cluster by terminating 28 Si DBs with H atoms was, however, a positive value of 0.24. This value is reduced as the cluster size is increased, but remains positive. Although the electronic charge may have been largely underestimated, this is a very strange result and contradicts the former neutral case. While electronic charges from the host SiO_2 spill over the H atom at the interstice, this transfer is reversed as the H and O atoms come closer. There still remains some uncertainty in real electronic charges for the H atom bonding to an O atom in the host SiO_2.

The H-atom migration from the initial O atom to the nearest neighbor, to the second-nearest neighbor, and to the two opposite site O atoms have been calculated, as shown in Fig. 2(a).[27] The energy barriers, final energy gains, and effective charges on the H atom at the saddle point are tabulated in Table I. All the effective charges even at the saddle points listed in Table I are negative values, implying that the effective charge at the H atom remains a negative value during migration processes. It reaches a lower value of -0.57 in the first-nearest case and of -0.61 in the opposite site 2 case, where the H atom comes closer to the middle of the interstice. The energy barrier for H migration to the nearest-neighbor O atom is found to be as low as 0.27 eV. If we add another H atom in this positively charged system, the interstitial H atom and the positively charged $(2Si{=}O{-}H)^{1+}$ complex have an attractive interaction with an energy of 0.6 eV. This is the direct evidence that the migrating H atom at an interstice is negatively charged

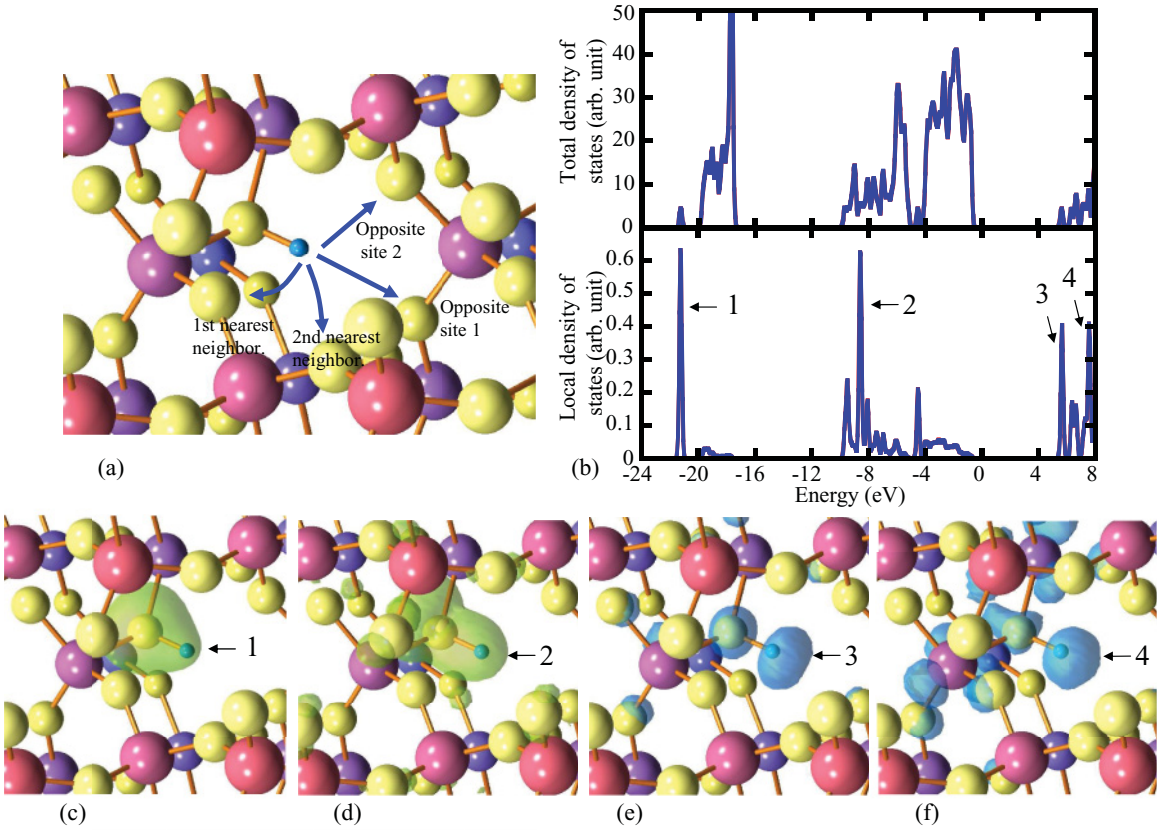

FIG. 2. (Color online) (a) Initial configuration for the H atom and migration paths in a positively charged $(\alpha\text{-quartz})^{1+}$. Large balls represent Si atoms from red to blue according to the depth. Small blue and white balls represent H and O atoms, respectively. (b) TDOS for the SiO_2 system (upper) and LDOS for the H atom (lower). Up- and down-spins are drawn by blue and red lines, respectively. (c), (d) Yellow and (e), (f) blue isosurfaces represent the electronic charges of states, corresponding to peaks 1, 2 and 3, 4 in (b), respectively.

even in the positively charged $(\alpha\text{-quartz})^{1+}$. As the distance between the two H atoms is more reduced to be 1 Å, however, this interaction turns into repulsion between the two H atoms. This is another implication that both H atoms are negatively charged. Since the H atom at the interstice of the host SiO_2 is negatively charged, H atoms migrate toward the lower energy anode in $(\alpha\text{-quartz})^{1+}$, corresponding to the polarity of applied bias voltage.

Now, we turn to H-atom migration in a negatively charged $(\alpha\text{-quartz})^{1-}$. Here, $(\alpha\text{-quartz})^{1-}$ denotes that one electron is added to the α-quartz. The negative charge has been compensated by a uniform positive background charge to avoid the divergence. The optimization of atomic positions leads to orbital hybridization of the H atom with one of the Si atoms in the host SiO_2, as shown in Fig. 3(a). Figure 3(b) shows the TDOS for the SiO_2 system (upper) and LDOS for the initial H atom (lower). The up- and down-spin states (blue lines) are fully degenerated and are hybridized with the host Si $3p$ states, as represented by the two peaks (1 and 2) located lower and higher than the top of the SiO_2 valence band in the LDOS. They correspond to the yellow isosurfaces of electronic charges of states at the H atom, as shown in Figs. 3(c) and 3(d), respectively. The effective charge on the H atom is a negative value of -0.79 because one electron is added to the system. The effective charge evaluated in the same atomic geometry of the central region in Fig. 3(a) by the Mulliken charges with the $(HSi_{18}O_{22})^{1-}$ cluster by terminating 28 Si DBs with H atoms was also a negative value of -0.27. The H-atom migration from the initial Si atom to the nearest neighbor, the second-nearest neighbor, and the opposite site Si atoms has been calculated, as shown in Fig. 3(a). The energy barriers, final energy gains, and effective charges on the H atom at

TABLE I. The energy barriers, final energy gains, and effective charges on the H atom at the saddle points for H-atom migration in $(\alpha\text{-quartz})^{1+}$.

Case	Energy barrier (eV)	Energy gain (eV)	Effective charge
1st nearest	0.93	−0.12	−0.57
2nd nearest	1.25	0.00	−0.46
opp. 1	0.27	−0.04	−0.31
opp. 2	0.37	0.05	−0.61

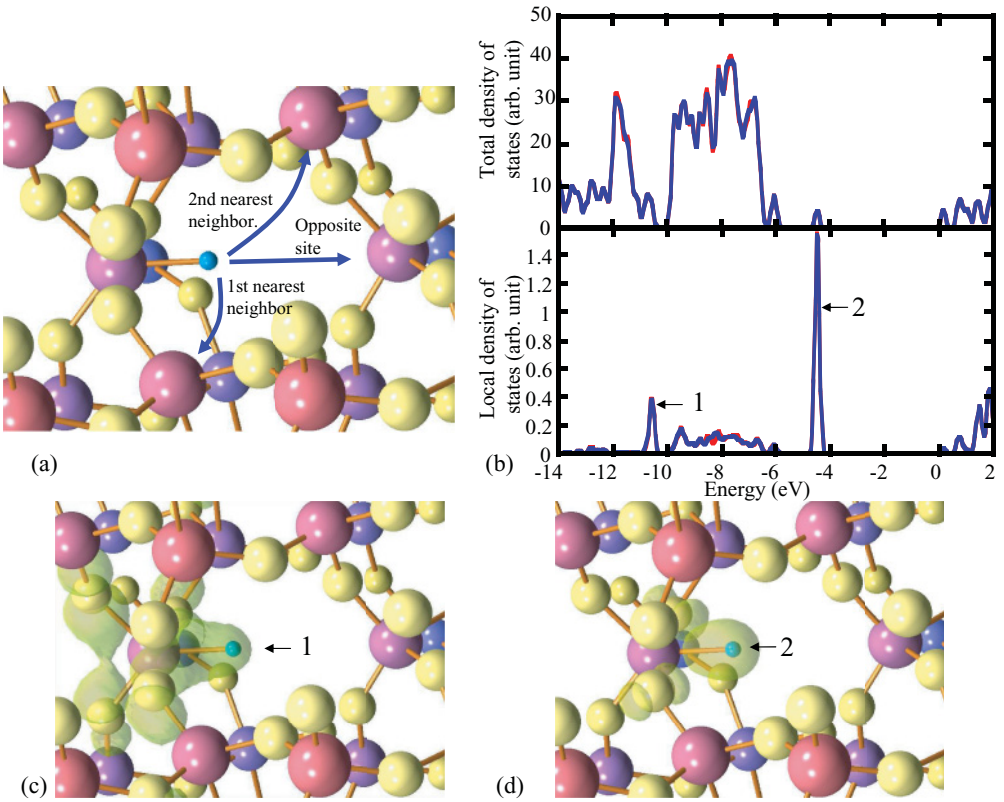

FIG. 3. (Color online) (a) Initial configuration for the H atom and migration paths in a negatively charged $(\alpha\text{-quartz})^{1-}$. Large balls represent Si atoms from red to blue according to the depth. Small blue and white balls represent H and O atoms, respectively. (b) TDOS for the SiO_2 system (upper) and LDOS for the H atom (lower). Up- and down-spin states are drawn by blue and red lines, respectively. (c), (d) Yellow isosurfaces represent the electronic charges of states corresponding to peaks 1 and 2 in (b).

the saddle point are tabulated in Table II. All the effective charges listed in Table II are negative values, implying that the effective charge at the H atom remains a negative value during migration processes. Although the energy barrier for H migration to the far Si site accompanied by H–Si bond breaking is an exceptionally high 2.35 eV, the normal H migration to the nearest-neighbor Si atom is found to be as low as 0.75 eV. H migration also occurs toward the lower energy anode side in $(\alpha\text{-quartz})^{1-}$ corresponding to the polarity of applied bias voltage when the temperature is high enough to assist H migration.

Although there still remains some uncertainty in real electronic charges for the H atom bonding to an O atom in the host SiO_2, we understand that, throughout these calculated results, the effective charge on the migrating H atom will be mostly negative irrespective of the Fermi-level position in the SiO_2 band gap. Hence, the H-atom migration will be directed toward the anode when the negative gate bias voltage is applied, corresponding well with the recent experimental findings on H-induced SiO_2 interface degradation for NBTI.[20]

When we tried to attach the second H atom to the 2Si=O–H complex in $(\alpha\text{-quartz})^{1+}$ or to the 4O≡Si–H complex in $(\alpha\text{-quartz})^{1-}$, the second H atoms moved away from the complex to the middle of the SiO_2 interstices. Neither the 2Si=O=2H complex nor the 3O≡Si=2H complex is stable in $(\alpha\text{-quartz})^{1+}$ and $(\alpha\text{-quartz})^{1-}$, respectively. Even when we added another hole or electron, those 2Si=O=2H complex and 3O≡Si=2H complex structures were not stable in $(\alpha\text{-quartz})^{2+}$ and $(\alpha\text{-quartz})^{2-}$, respectively. Each added H atom instead attached to a different O atom by forming another 2Si=O–H complex in $(\alpha\text{-quartz})^{2+}$ or to a different Si atom by forming another 4O≡Si–H in $(\alpha\text{-quartz})^{2-}$. This suggests that O vacancy generation cannot be triggered by H atoms and that it does not lead to degradation of crystal SiO_2 structures with no defect even if another electron or hole is introduced.

TABLE II. The energy barriers, final energy gains, and effective charges on the H atom at the saddle points for H-atom migration in $(\alpha\text{-quartz})^{1-}$.

Case	Energy barrier (eV)	Energy gain (eV)	Effective charge
1st nearest	0.75	−0.03	−0.88
2nd nearest	1.16	0.05	−0.90
opp. 1	2.35	0.05	−0.71

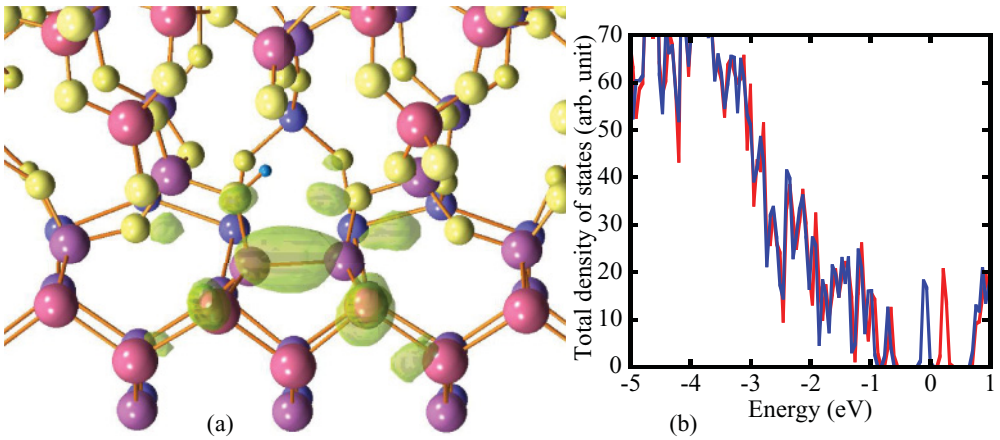

FIG. 4. (Color online) (a) The equilibrium position of the H atom in a SiO_2/Si interface. Large balls represent Si atoms from red to blue according to the depth. Small blue and white balls represent H and O atoms, respectively. Yellow isosurface represents the electronic charges of states located below the bottom of the Si conduction band. (b) TDOS for the SiO_2/Si system. Up- and down-spin states are drawn by blue and red lines, respectively.

B. H migration in SiO_2/Si interface

The equilibrium position of a H atom in a SiO_2/Si interface after geometry optimization results in orbital hybridization with an O atom in the host SiO_2/Si[17] irrespective of charge state in the SiO_2/Si system. The most stable charge state at the 2Si=O–H complex is realized through charge transfer between the SiO_2 layer and the Si substrate, which is a carrier reservoir. This is because the bulk Si has a substantially lower band gap compared with the SiO_2. The calculations in this subsection were, therefore, performed under a neutral charge state.

A SiO_2/Si interface structure is prepared by inserting an O atom into a Si–Si bond on a repeated slab, where a single Si atom is removed beforehand to form a wide interstice space to evaluate adsorption energy accurately. Figure 4(a) shows a typical SiO_2/Si system of the threefold O atom bonding with a H atom, being realized through geometry optimization. The yellow isosurface displays the electronic charge of the occupied state located in the Si band gap. Figure 4(b) shows the TDOS for the SiO_2/Si system. The up-spin state (blue lines) isolated in the Si band gap is occupied, corresponding to the yellow isosurface, whereas the down-spin state (red lines) is unoccupied. The 2Si=O–H complex with the threefold O atom in Fig. 4(a) must be positively charged because of the expulsion of one electron. The expelled electron has moved into the Si substrate accordingly, as displayed by the yellow isosurface. This state energy is lowered from the Si conduction band to the isolated state in the Si band gap through strong Coulomb attraction between the positively charged $(2Si{=}O{-}H)^{1+}$ complex and its negative electronic charge. This reaction occurs exothermally because the 2Si=O–H complex gains energy by forming the O–H bond larger than the small excitation energy over the Si band gap needed for expelling one electron. The excitation energy is, furthermore, reduced by Coulomb attraction between the positively charged $(2Si{=}O{-}H)^{1+}$ and the electron. At almost all O sites in the present SiO_2/Si interface system, orbital hybridization of a H atom with an O atom can be found, leaving an extra electron in the Si substrate. Provided SiO_2 layer thickness below the H atom is thin enough, electron tunneling occurs through a SiO_2 layer. This understanding is applicable to whole O atoms in a SiO_2/Si interface system. The optimized geometry of a $(2Si{=}O{-}H)^{1+}$ complex will be generated provided the underlying SiO_2 layer is thin enough for electron tunneling. The effect of the other supercells to the $(2Si{=}O{-}H)^{1+}$ complex formation was also calculated to be the small repulsion energy of 0.02 eV, making no difference to the results.

The initial configuration of a H atom bonding to an O atom in the SiO_2/Si interface and the migration paths for the H atom toward the nearest neighbors and the opposite sites O atoms are drawn in Fig. 5(a). Figure 5(b) shows the TDOS for the SiO_2/Si system (upper) and LDOS for the initial H atom (lower). The up- and down-spin states (blue and red lines) are fully degenerated except for isolated states in the Si band gap. The occupied states in the LDOS are split into almost seven peaks through hybridization with the host O states. The electronic charges of states at the H atom corresponding to the main two peaks (1 and 2) are displayed by yellow isosurfaces in Figs. 5(c) and 5(d), respectively. These hybridized states are mostly located at the energies much lower than the top of the SiO_2 valence band. The peaks located at -24 eV and at -13 eV from the Fermi level are lower than the O 2s states and the O 2p states, respectively, because the positively charged 2Si=O–H complex further lowers the electronic states at the H atom, as in the case of $(\alpha\text{-quartz})^{1+}$. On the other hand, the electronic charges of states at the H atom for the two unoccupied states (peaks 3 and 4) are displayed by blue isosurfaces in Figs. 5(e) and 5(f), respectively, clearly indicating that these states are antibonding states between the H 1s and O 2s states, and between the H 1s and O 2p states. The effective charge on the H atom in this case is also evaluated to be still a negative value of -0.47. This value may also have been negatively overestimated because of the small H atom. Hence, integration of the LDOS along energy for both spins is calculated to be 2.44, larger than 2.0, implying the other atomic orbital components. By comparing the occupied components of 1.47 and the unoccupied components of 0.97, the effective charge of the H atom seems to be still negative, where the components from the other orbits are considered

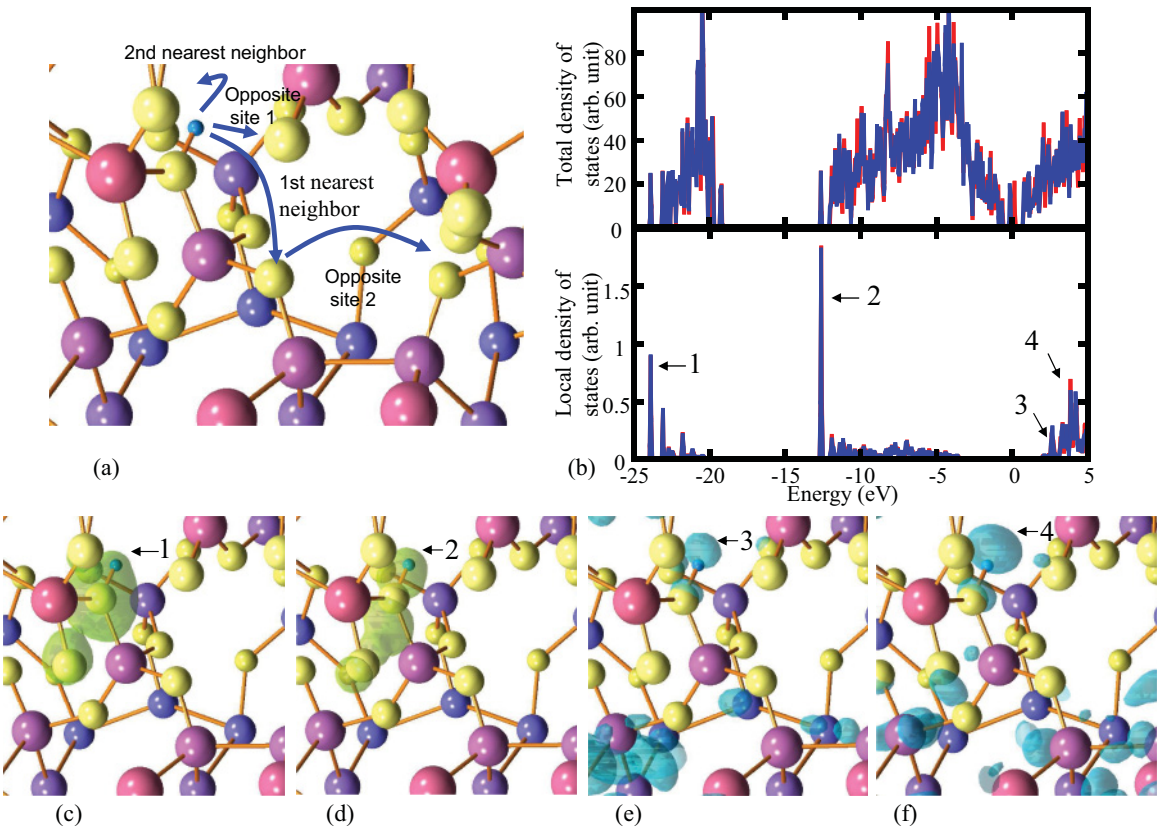

FIG. 5. (Color online) (a) Initial configuration for the H atom and migration paths in a SiO_2/Si interface. Large balls represent Si atoms from red to blue according to the depth. Small blue and white balls represent H and O atoms, respectively. (b) TDOS for the SiO_2 system (upper) and LDOS for the H atom (lower). Up- and down-spin states are drawn by blue and red lines, respectively. (c), (d) Yellow and (e), (f) blue isosurfaces represent the electronic charges of states, corresponding to peaks 1, 2 and 3, 4 in (b), respectively.

to be involved at almost the same rate. Since the 2Si=O–H complex is positively charged, the electronic configuration of this case is very close to $(\alpha\text{-quartz})^{1+}$. Electronic charge transfer from the SiO_2 system to the H atom is also possible in this case.

Since the Wigner-Seitz cell may sometimes overestimate the effective charge of the H atom by counting the electronic charges of surrounding atoms, we first calculated the effective charge on a small cluster of $(2Si{=}O{-}H)^{1+}$. We chose this cluster because the effective charge evaluation of the H atoms with Wigner-Seitz cells is not affected by charges from the opposite side atoms. The effective charge on the H atom is thus calculated to be −0.30, which is close to the result of −0.47 for Fig. 5. The Mulliken charge is, however, 0.39 in this case. Then, the effective charge has been additionally calculated in the same atomic geometry of Fig. 4(a) with the $HSi_{55}O_{37}$ cluster by terminating 60 Si DBs with H atoms. The effective charge evaluated by Mulliken charges for the same geometry is, however, 0.27 in this case. Although the difference in the effective charges comes closer as the cluster size is enlarged, there still remains some uncertainty in real electronic charges.

The energy barriers, final energy gains, and effective charges on the H atom at the saddle point are tabulated in Table III. The energy barriers are found be almost 1.0 eV at most. The extra electron is always expelled into the Si substrate during the H-atom migration, as indicated by the isolated state in the Si band gap [Fig. 4(a)]. All the effective charges listed in Table III are also negative values. Although the most negative value in this case is −0.55, the effective charge reaches the minimum value of −0.71 as the H atom moves to the midcenter of the interstice because electrons can be supplied from the Si substrate. The effective charge evaluated by the Mulliken

TABLE III. The energy barriers, final energy gains, and effective charges on the H atom at the saddle points for H-atom migration in SiO_2/Si interface.

Case	Energy barrier (eV)	Energy gain (eV)	Effective charge
1st nearest	1.01	−0.39	−0.47
2nd nearest	0.77	0.23	−0.55
opp. 1	0.52	0.23	−0.37
opp. 2	0.51	−0.62	−0.31

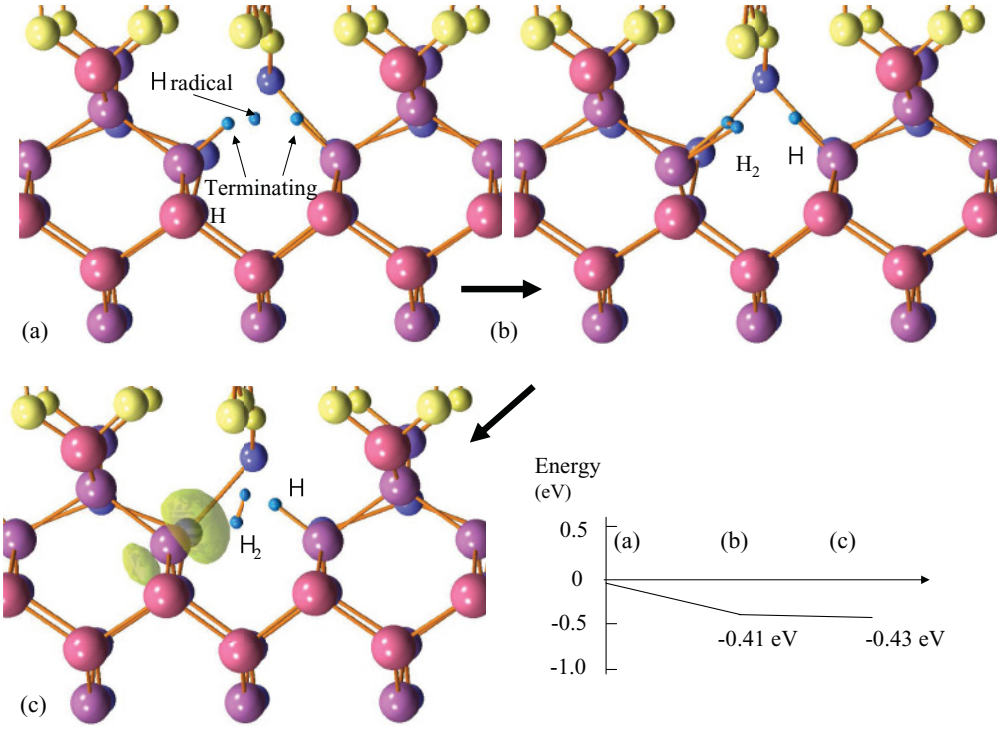

FIG. 6. (Color online) H-atom-terminated SiO_2/Si interface defect and trajectory of another H atom forming again a H_2 molecule from (a) the initial configuration, to (b) the H_2 molecule desorbing stage, and to (c) the final configuration. Large balls represent Si atoms from red to blue according to the depth. Small blue and white balls represent H and O atoms, respectively. Yellow isosurfaces represent the electronic charges of the DB.

charge for the H atom at the midcenter of the interstice with the $HSi_{55}O_{37}$ cluster also turns out to be a negative value of -0.05, suggesting that the effective charge of the migrating H atom is definitely negative. As described in the former subsection, the negatively charged H atoms will also migrate toward the lower energy anode side in SiO_2/Si systems corresponding to the polarity of applied bias voltage when the temperature is high enough to assist H-atom migration.

C. SiO_2 degradation through O vacancy generation by H atoms in SiO_2/Si interface

When the SiO_2 film formed on the Si substrate is negatively biased from the gate electrode, negatively charged H atoms incorporated into SiO_2 film migrate toward the Si substrate, tending to accumulate at SiO_2/Si interfaces. We explored H-induced degradation of H-terminated interface defects and degradation of SiO_2 layers.

An interface defect consisting of two weakly binding DBs is frequently generated just below a SiO_2/Si interface through Si interstitial formation as a consequence of stress accumulation along the lateral direction during Si oxidation.[11,23] Under annealing in hydrogen ambient, a H_2 molecule diffusing at the SiO_2/Si interface will dissociate over the DBs, and the dissociated H atoms terminate DBs at the SiO_2/Si interface defects.[10] Figure 6 shows a typical H-terminated SiO_2/Si interface defect and the trajectory of another H atom to form again a H_2 molecule. When another H atom migrates from the SiO_2 layer to the H-terminated defect [Fig. 6(a)], the H atom forms a H_2 molecule together with a hydrogen atom terminating the DB at the defect with an energy gain of 0.41 eV from the geometry (a) to (b) [Fig. 6(b)]. This H_2 molecule is desorbed from the interface defect with an energy gain of 0.02 eV from the geometry (b) to (c), leaving an exposed Si DB behind as displayed by yellow isosurfaces [Fig. 6(c)]. Degradation of hydrogen termination of interface defects thus occurs.

When one H atom, migrating toward the 2Si=O–H complex, arrives at the H atom, as shown in Fig. 7(a), a H_2 molecule is generated through bond reformation between the two H atoms, breaking the initial H–O bond. This is because the H–H bond is stronger than the H–O bond at the 2Si=O–H complex. This reaction occurs without energy barrier.

Let us consider another scenario. We assume that two H atoms are adsorbed at the O atoms next nearest each other [Fig. 7(a)]. The yellow isosurface displays the electronic charges of the states expelled through threefold coordination of the O atom. Up- and down-spin states were degenerated in the yellow isosurface, as depicted in Figs. 7(a) to 7(b). When the H atom at the left side migrates toward the 2Si=O–H complex at the right side [Fig. 7(a)], it forms a bond with the O atom, breaking a single Si–O backbond in the 2Si=O–H complex because the H–O bond is stronger than the Si–O bond at the 2Si=O–H complex [Fig. 7(b)]. The reaction occurs with an energy barrier of 1.17 eV from the geometry (a) to (b). The 2Si=O–H complex is reformulated as a Si–O=2H complex and a Si DB. Then, another H atom arrives at the same O atom adjacent to the Si–O=2H complex [Fig. 7(c)]. Up- and down-spin states occupy the dark yellow isosurface whereas the bright yellow DB is occupied by a single electron much closer to the Fermi level.

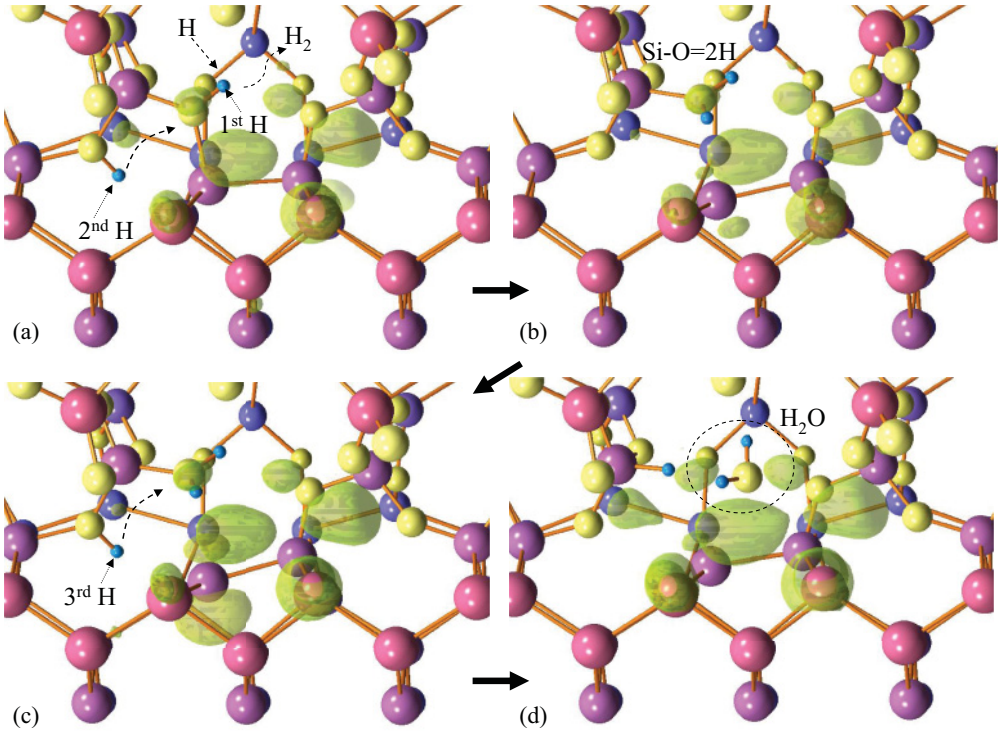

FIG. 7. (Color online) H-atom-bonded SiO_2/Si interface and trajectory of H_2O desorption induced by another H atom from (a) the initial configuration, to (b) H_2O formation stage, and to (c) H_2O desorbing stage induced by the other H atom, and to (d) the final configuration. Large balls represent Si atoms from red to blue according to the depth. Small blue and white balls represent H and O atoms, respectively. Yellow isosurfaces represent the electronic charges of the expelled electron and DBs.

When the H atom migrates in between the remaining Si–O bond, the H atom makes a bond with the Si atom, breaking another Si–O backbond [Fig. 7(d)] because the Si–H bond is stronger than the Si–O bond at the Si–O=2H complex. This reaction occurs with an energy barrier of 1.09 eV from the geometry (c) to (d). Consequently, the O atom returns to the initial twofold coordination with the two H atoms from the threefold coordination after receiving the expelled electron from the Si substrate. Accordingly, the doubly occupied states in the band gap disappeared. As a result, a H_2O molecule desorbed from the SiO_2 network, leaving an O vacancy behind in the SiO_2 film. These process sequences from (a) to (b) and from (c) to (d) occur with slight energy gains, and the geometry (d) falls further into a lower energy configuration. The 2Si=O–H complex formation and the H_2O desorption triggered by arriving H atoms thus occur exothermally with electron transfer to and from the Si substrate. After O vacancy generation, exposed Si DBs work as negatively charged traps following electron injection.[13,20]

The H_2O desorption occurs not only at the SiO_2/Si interface, but also inside the SiO_2 network provided electron tunneling occurs between the 2Si=O–H complex and the Si substrate. Desorption probability of H_2O at each site will be evaluated by the bond strength between the initial H atom and the O atom at the 2Si=O–H complex. This is because the weakly bonding H atom is more likely to be desorbed as a H_2 molecule by breaking the weaker H–O bond when another H atom arrives. Consequently, the 2Si=O–H complex disappears. Figure 8 shows typical 2Si=O–H complexes located at each site and their H–O binding energies, where (a) the O atom is bonding to a Si atom with a DB at the SiO_2/Si interface, (b) the O atom is bonding to Si atoms with no DB at the SiO_2/Si interface, (c) the O atom is in a SiO_2 network in the SiO_2 layer, and (d) the O atom is terminating Si DBs at the SiO_2/Si interface defect. The H-O binding energy was evaluated by the energy difference between the optimized geometry for all the atom positions and the geometry with an H-O distance of 1.8 Å. This is because the further elongation of the H-O distance introduces the interactions from the other atoms. The binding energy between H and O atoms tends to be reduced from the highest value of 3.37 eV for case (a) to 2.66 eV for case (b), to 2.11 eV for case (c), and to 1.70 eV for case (d). From the calculated results, we learn that a H_2O molecule is most likely to be generated from SiO_2/Si interfaces with a DB, where the strong dipole interaction is working between the positively charged $(2Si{=}O{-}H)^{1+}$ complex and the excess electron at the DB belonging to the same 2Si=O–H complex, and that it is possible for a H_2O molecule formation inside the SiO_2 network or the O-terminated interface defect to occur but with much lower probability. This implication of the degradation growing from the SiO_2/Si interface corresponds well with the recent experimental results that H-induced degradation of gate stacks strongly depends on the underlying interface SiO_2 layer thickness.[20]

IV. DISCUSSION

In the present study, we showed that H_2O desorption occurs from the SiO_2 network in SiO_2/Si interfaces, in accordance

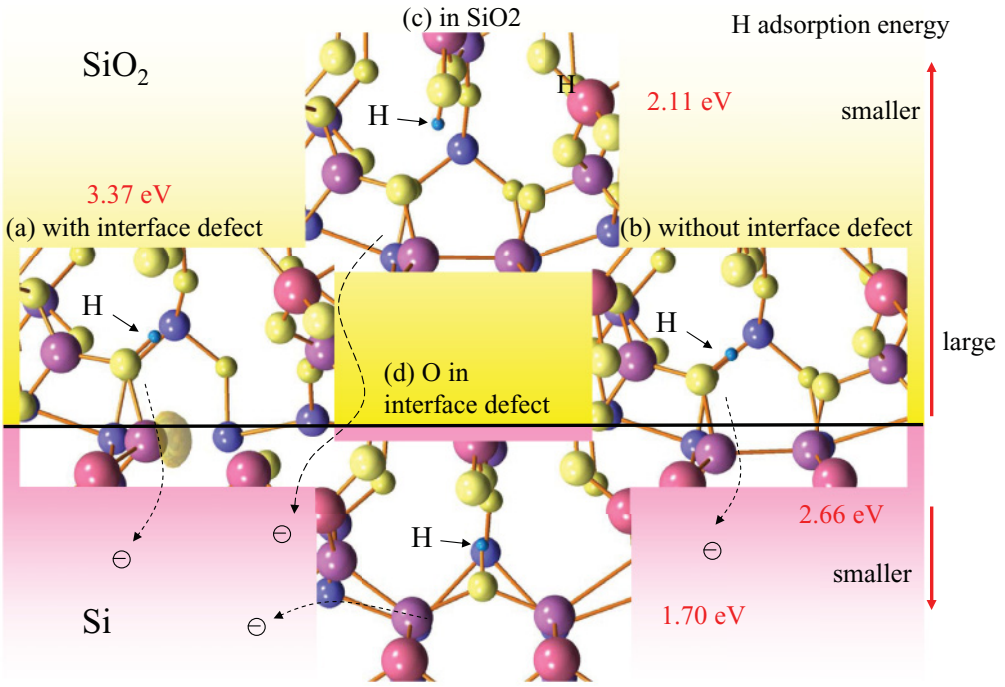

FIG. 8. (Color online) H-terminated O sites and H-O binding energies where the O atom is (a) bonding with a Si atom with a DB at the SiO_2/Si interface, (b) bonding with Si atoms with no DB at the SiO_2/Si interface, (c) in a SiO_2 network above the SiO_2/Si interface, and (d) bonding with Si atoms at the SiO_2/Si interface defect. Large balls represent Si atoms from red to blue according to the depth. Small blue and white balls represent H and O atoms, respectively. Yellow isosurfaces represent electronic charges of the DBs.

with the following steps:

$$\begin{aligned} 2\text{Si}{=}\text{O} + \text{H} &\rightarrow 2\text{Si}{=}\text{O}{-}\text{H}, \\ 2\text{Si}{=}\text{O}{-}\text{H} + \text{H} &\rightarrow \text{Si}{-}\text{O}{=}2\text{H} + \text{Si}{-}, \\ \text{Si}{-}\text{O}{=}2\text{H} + \text{H} &\rightarrow \text{Si}{-}\text{H} + \text{H}_2\text{O}. \end{aligned} \quad (1)$$

This reaction can be reversed by H_2 desorption (preventing reaction) after the first step as

$$2\text{Si}{=}\text{O}{-}\text{H} + \text{H} \rightarrow 2\text{Si}{=}\text{O} + \text{H}_2, \quad (2)$$

where the binding energy of a H_2 molecule is larger than that of the H–O bond at the 2Si=O–H. Then, the geometry reverts to the original positions. These are typical H_2O desorption and H_2 desorption processes. For the H_2O desorption processes, there is another reaction path after the first step, which is

$$\begin{aligned} 2\text{Si}{=}\text{O}{-}\text{H} + \text{H} &\rightarrow \text{Si}{-}\text{H} + \text{Si}{-}\text{O}{-}\text{H}, \\ \text{Si}{-}\text{O}{-}\text{H} + \text{H} &\rightarrow \text{Si}{-}\text{O}{=}2\text{H}, \\ \text{Si}{-}\text{O}{=}2\text{H} + \text{H} &\rightarrow \text{Si}{-}\text{H} + \text{H}_2\text{O}. \end{aligned} \quad (3)$$

For preventing reactions, there is yet another reaction path,

$$\text{Si}{-}\text{O}{=}2\text{H} + \text{H} \rightarrow \text{Si}{-}\text{O}{-}\text{H} + \text{H}_2. \quad (4)$$

These reactions are also found to occur exothermically. Since all the reactions are exothermic except for H migration and adsorption, the probability of the reactions will not be more dependent on process sequences but will be largely determined by the trajectory of H-atom migration. The bond breaking in chemical reactions is most likely to occur owning to a weaker bond because migrating H atoms easily induce the O–H bond breaking and create a H_2 molecule (preventing reaction).

As negative gate bias is applied, H atoms in the SiO_2 layer fabricated on the Si substrate will migrate toward the SiO_2/Si interface. H_2O desorption is likely to occur where the preventing reaction does not occur easily. We understand that the desorption of H_2O is most likely to occur from the SiO_2/Si interface with a DB, and that it is still possible for the desorption of a H_2O molecule inside the SiO_2 networks or from O-terminating interface defects to occur but with lower probability (Fig. 8). Since the O vacancy formation process is most likely to occur just at the SiO_2/Si interface, the SiO_2/Si interface moves gradually into SiO_2 networks after O vacancy formation. On the other hand, when an O vacancy is generated in the SiO_2 networks, the O vacancy will migrate toward the cathode because the O atom is negatively charged in the SiO_2 networks. Under the negative gate voltages, the generated O vacancy migrates toward the gate electrode because the migration will be thermally assisted. The degradation of SiO_2 will thus spread from the SiO_2/Si interface region to the bulk SiO_2 film, leading to the electrical breakdown of insulation of SiO_2 films.

A strange paradox remains concerning H-atom migration in SiO_2/Si interfaces. Although H atoms are negatively charged, the 2Si=O–H complex surrounding the migrating H atom must be positively charged. This means that, in accordance with the negatively charged H-atom migration toward the anode side, the positively charged complex must follow the negatively charged H-atom migration to the anode side, resulting in the total energy increase. It may happen since the positively charged complex migration occurs as a consequence of the total energy relaxation after the H-atom migration. In actual cases, however, it may be that electrons traveling from the

cathode to the anode compensate this positively charged complex migration rather than that the extra electrons expelled into the Si substrate return to the SiO_2 layer in SiO_2/Si interfaces as described in the former section.

V. CONCLUSION

We examined H-atom migration behaviors in SiO_2/Si systems, which are dependent on the charge-state polarity of the SiO_2 systems. Although there still remains some uncertainty in real electronic charges for the H atom bonding to an O atom in the host SiO_2, the migrating H atom is mostly negatively charged irrespective of the charge-state polarity, indicating gate bias polarity dependent H-atom migration toward the anode side. Proton transfer must always be accompanied by electronic charges. The migration of the H atom in the SiO_2 systems with no defect generates no O vacancy irrespective of charge-state polarity in the SiO_2 systems. In the SiO_2/Si systems, however, H atoms are orbital hybridized with O atoms by forming threefold coordination as the H atoms migrate toward the SiO_2/Si interface. The excess electron is adsorbed in the Si substrate, resulting in electron transfer from the 2Si=O–H complex to the Si substrate. The Coulomb attraction generated between the excess electron and the positively charged 2Si=O–H complex enhances the H–O bond strength. H_2O desorption is, therefore, likely to be induced from the SiO_2/Si interface with a DB by alternate electron transfer between the 2Si=O–H complex and the Si substrate. Accumulation of the O-atom vacancy generation leads to the electrical breakdown of the SiO_2 film, which agrees well with the recently found gate bias polarity dependent breakdown of SiO_2 films.

ACKNOWLEDGMENTS

The authors would like to thank Y. Mitani, I. Hirano, Y. Nakasaki, T. Yamasaki, and T. Uda for their support and discussion.

*kato@arl.rdc.toshiba.co.jp

[1] D. J. Dimaria and J. W. Stasiak, J. Appl. Phys. **65**, 2342 (1989).
[2] P. M. Lenahan and P. V. Dressendorter, J. Appl. Phys. **55**, 3495 (1984).
[3] K. Kato, T. Yamasaki, and T. Uda, Phys. Rev. B **73**, 073302 (2006).
[4] A. Stirling, A. Pasquarello, J.-C. Charlier, and R. Car, Phys. Rev. Lett. **85**, 2773 (2000).
[5] A. Stesmans and V. V. Afanas'ev, J. Appl. Phys. **83**, 2449 (1998).
[6] P. E. Blochl and J. H. Stathis, Phys. Rev. Lett. **83**, 372 (1999).
[7] J. H. Stathis and E. Cartier, Appl. Phys. Lett. **63**, 1510 (1993).
[8] E. Cartier, J. H. Stathis, and D. A. Buchanan, Appl. Phys. Lett. **63**, 1510 (1993).
[9] K. Kato, H. Kajiyama, S. Heike, T. Hashizume, and T. Uda, Phys. Rev. Lett. **86**, 2842 (2001).
[10] M. L. Read and J. D. Plummer, J. Appl. Phys. Rev. **63**, 5776 (1988).
[11] T. Ishihara, D. Matsushita, and K. Kato, IEDM Tech. Dig. 75 (2009); T. Ishihara, D. Matsushita, K. Tatsumura, Y. Nakabayashi, J. Koga, and K. Kato, *ibid*. 101 (2007).
[12] Chih-Tang Sah, J. Yuan-Chen Sun, and J. Jeng-Tao Tzou, J. Appl. Phys. **55**, 1525 (1984).
[13] Y. Nissan-Cohen and T. Gorczyca, IEEE Electron Devices Lett. **9**, 287 (1989).
[14] A. Yokozawa and Y. Miyamoto, Phys. Rev. B **55**, 13783 (1997).
[15] K. Xiong and J. Robertson, J. Appl. Phys. **102**, 083710 (2007).
[16] J. Godet, P. Broqvist, and A. Pasquarello, Appl. Phys. Lett. **91**, 262901 (2007).
[17] A. H. Edwards, P. A. Schultz, and H. P. Hjalmarson, Phys. Rev. B **69**, 125318 (2004).
[18] P. Broqvist, A. Alkauskas, J. Godet, and A. Pasquarello, J. Appl. Phys. **105**, 061603 (2009).
[19] Chris G. Van de Walle, IEDM Tech. Dig. 16.4 (2005).
[20] I. Hirano, K. Kato, Y. Nakasaki, S. Fukatsu, K. Sekine, M. Goto, S. Inumiya, M. Sato, and Y. Mitani, Int. Rel. Phys. Symp. 424 (2010); I. Hirano, Y. Nakasaki, S. Fukatsu, A. Masada, and Y. Mitani, *ibid*. 355 (2009).
[21] A. Bongiorno, L. Colombo, and F. Cargnoni, Chem. Phys. Lett. **264**, 435 (1997).
[22] P. W. Peacock and J. Robertson, Appl. Phys. Lett. **83**, 2025 (2003).
[23] K. Kato, I. Hirano, Y. Nakasaki, and Y. Mitani, Proceedings of the ICPS-30, 961 (2011).
[24] K. Kato, D. Matsushita, K. Muraoka, and Y. Nakasaki, Phys. Rev. B **78**, 085321 (2008).
[25] PHASE, Institute of Industrial Science, University of Tokyo, [http://www.ciss.iis.u-tokyo.ac.jp/english/].
[26] D. Vanderbilt, Phys. Rev. B **41**, 7892 (1990).
[27] J. Godet and A. Pasquarello, Phys. Rev. Lett. **97**, 155901 (2006).